

**PCCP****Fermi Resonance Controlled Product Branching in the  
H+HOD reaction**

Journal:	<i>Physical Chemistry Chemical Physics</i>
Manuscript ID	CP-ART-04-2018-002279.R1
Article Type:	Paper
Date Submitted by the Author:	15-May-2018
Complete List of Authors:	Zhao, Bin; Universität Bielefeld, Fakultät für Chemie Manthe, Uwe; Universität Bielefeld Universitätsstr. 25,, Theoretische Chemie, Fakultät für Chemie Guo, Hua; University of New Mexico, Department of Chemistry

SCHOLARONE™  
Manuscripts

## Fermi Resonance Controlled Product Branching in the H+HOD reaction

Bin Zhao<sup>1,2,\*</sup>, Uwe Manthe<sup>1</sup>, and Hua Guo<sup>2</sup>

<sup>1</sup>*Theoretische Chemie, Fakultät für Chemie, Universität Bielefeld, Universitätsstr. 25, D-33615 Bielefeld, Germany*

<sup>2</sup>*Department of Chemistry and Chemical Biology, University of New Mexico, Albuquerque, New Mexico 87131, USA*

\* Corresponding author: [bin.zhao@uni-bielefeld.de](mailto:bin.zhao@uni-bielefeld.de)

## Abstract

Accurate full-dimensional quantum state-to-state reaction probabilities and integral cross sections are calculated for the title reaction. Product vibrational state distributions are studied for the HOD reactant in various vibrational states. The correlation of initial reactant vibrational excitation with product channel branching and product vibrational state distribution is analyzed in detail. In particular, the effect of bending vibrational excitation on the reactivity is studied. While results for the HOD reactant in the fundamentally excited bending vibrational state confirm intuitive expectation with minor enhancement for both product channels, a surprising effect is found for HOD in the first overtone of bending vibration. Here, the reactivity towards breaking the OD bond is significantly enhanced. This finding can be explained by the state-mixing caused by a 1:2 Fermi resonance between the fundamental OD stretch and the first overtone of the bend. The results highlight the importance of a proper analysis of the initial vibrational state.

## I. Introduction

Control of a polyatomic chemical reaction towards a desired product channel by selective excitation of a reactant mode has been a holy grail for physical chemists.<sup>1-3</sup> The four-atom A+BCD reaction represents the smallest system that supports multiple vibrational modes in the reactant and thus has received a lot of attention.<sup>4-8</sup> Specifically, the HOD reactant in the title reaction has three distinctive vibrational modes: the OD stretch ( $\nu_{OD}$ ), the OH stretch ( $\nu_{OH}$ ), and the bend ( $\nu_b$ ). Four reactive channels exist for the title reaction,



where the first two are abstraction channels and the other two are exchange channels. The abstraction channels, which have a lower reaction threshold, are studied in the present work. With one of the hydrogens replaced by deuterium, the two abstraction product channels can be distinguished experimentally.

The  $H + H_2O \leftrightarrow H_2 + OH$  reaction and its isotopologues have been studied intensively by experiments<sup>9-19</sup> and full-dimensional theory,<sup>20-46</sup> but the number of detailed investigations studying state-to-state differential cross sections is still limited.<sup>17-19, 47-52</sup> For the title reaction, pioneering work<sup>9-13</sup> studied the branching ratio between the (A1) and (A2) channels. The first experiment reported by Crim and coworkers<sup>9, 10</sup> revealed strong bond selectivity towards the  $H_2 + OD$  product channel in the reaction of thermal H

atoms with the HOD molecules excited to the  $\nu_{\text{OH}}=4$  vibrational state, while in the reaction of thermal H atoms with HOD prepared in the  $\nu_{\text{OD}}=5$  vibrational state, only products corresponding to the other channel, i.e., HD + OH, were observed.<sup>11</sup> In these experiments, the HOD reactant was prepared in highly excited vibrational states and the internal energy exceeded the reaction barrier ( $\sim 0.9$  eV) so that it could react with the thermal H atom. On the other hand, Zare and coworkers studied the reaction of fast H atoms with HOD molecules in the  $\nu_{\text{OD}}=1$  and  $\nu_{\text{OH}}=1$  vibrational states.<sup>12, 13</sup> At a collision energy of 1.5 eV, strong bond selectivity was also found despite the fact that the internal energy initially deposited in the HOD reactant was only 18% and 23% of the total energy, respectively. The experimental branching ratio of the two abstraction channels has been qualitatively reproduced by theoretical calculations employing the quasi-classical trajectory,<sup>53</sup> reduced-dimensional<sup>54-56</sup> and full-dimensional<sup>29</sup> quantum wave packet methods.

The excitation of the bending vibration of the water reactant is expected to be less efficient in promoting the title reaction and its isotopologues, as it is not directly coupled to the bond cleavage coordinates. Indeed, Crim and coworkers<sup>10</sup> demonstrated that excitation to the  $|02\rangle|2\rangle$  state of the  $\text{H}_2\text{O}$  reactant was much less efficient in promoting the reaction than excitation to the  $|03\rangle|0\rangle$  state when one quantum of the OH stretching was replaced with two quanta of bending in similar energies. Here, the first two quantum numbers denote the two local stretching mode of  $\text{H}_2\text{O}$  and the third one the bending mode. Zare and coworkers<sup>15</sup> discovered in the  $\text{H} + \text{D}_2\text{O}$  reaction that one quantum of bending excitation had no enhancement effect.

The results described above are in agreement with intuitive expectations and can be readily understood in terms of the Sudden Vector Projection (SVP) model.<sup>57</sup> In the SVP model, the access to the reactive transition state is assumed to be sudden so that the vibrational excitation in the reactant has no time to redistribute to other modes. When this criterion is satisfied, the ability of a reactant vibrational mode to promote the reaction can be attributed to its coupling with the reaction coordinate at the transition state, which can be approximately quantified by the overlap between the vibrational normal mode vector with the reaction coordinate vector. The larger the overlap, the stronger the coupling with the reaction coordinate, and thus the higher the ability to promote the reaction. This intuitive transition-state based model, which can be thought as an extension of Polanyi's rules,<sup>58</sup> has been tested in many reactive systems and found to be quite robust.<sup>59, 60</sup>

In a recent communication,<sup>61</sup> a counterintuitive scenario for the mode specificity has been found studying the  $\text{H} + \text{CHD}_3 \rightarrow \text{H}_2 + \text{CD}_3$  reaction. Like the title reaction, vibrational excitation of the CH stretching mode is expected to strongly promote the reaction. Vibrational energy deposited in other vibrational modes should not yield a promoting effect at a comparable level.<sup>62</sup> In contrast to intuitive expectation, significant enhancement of the reactivity was found when the  $\text{CD}_3$  umbrella-bending vibration was prepared in its second overtone state. The interesting discovery was rationalized by a Fermi-resonance type mixing of the second overtone of the  $\text{CD}_3$  umbrella-bend with the CH stretching fundamental, an effect that was called 'reactivity borrowing'. We note in passing that the effect of the Fermi resonance on the product branching was not discussed in Ref. 61.

In the present work, accurate state-to-state calculations for the title reaction will be presented. The correlation of the vibrational excitation of the HOD reactant with the product channel branching and product vibrational state distributions will be analyzed. Most importantly, it will be demonstrated that the 1:2 Fermi resonance between the fundamental OD stretching and first overtone bending modes strongly affects the product branching ratio and controls the product vibrational state distribution.

This publication is organized as follows. The next section (Sec. II) outlines the theoretical approach and numerical details. The results are presented and discussed in Sec. III. The conclusions are given in Sec. IV.

## II. Theory and Numerical Details

A reactant-coordinate based (RCB) method<sup>51, 63, 64</sup> is employed in the study of state-to-state quantum reactive scattering of the title reaction. The details of the method have been described elsewhere<sup>51</sup> and only a brief introduction is given here. The initial wave packet, prepared in the reactant asymptotic region in a specific vibrational eigenstate of the HOD reactant, is propagated with the second-order split operator method<sup>65</sup> to the product asymptotic region using exclusively the H + HOD reactant Jacobi coordinate system. The product quantum state resolution is realized on a dividing surface defined in either the H<sub>2</sub> + OD or the HD + OH product arrangement by projecting out the contributions of all the ro-vibrational states from the energy eigenfunction after a time-energy Fourier transform. An accurate neural network based potential energy surface (PES) of the H<sub>3</sub>O system<sup>66</sup> is used in the calculations with the same parameters reported in Ref. 52 (also listed in Table S-I of ESI). It should be noted that although the OD and OH bonds of the HOD reactant are both reactive, the calculations here pre-select only one

to be reactive and treat the other as non-reacting. This approximation has been proven to be very accurate in the abstraction channels because the two corresponding transition states of the two product channels are well separated and no reactive flux accesses both transition states during the reaction.<sup>32, 45</sup> For the sake of simplicity, two independent calculations are thus performed separately for the two individual product channels.

### III. Results and discussion

The branching ratio between channels (A1) and (A2) depends on the vibrational excitation of the HOD reactant. To illustrate this effect, total reaction probabilities for zero total angular momentum ( $J_{\text{tot}}=0$ ) are shown on the left column of Fig. 1. The initial vibrational states of the HOD reactant in the ground rotational state are denoted as  $(\nu_{\text{OD}}, \nu_{\text{b}}, \nu_{\text{OH}})$ , where  $\nu_{\text{OD}}$ ,  $\nu_{\text{b}}$ ,  $\nu_{\text{OH}}$  are the quantum numbers of the OD stretching, bending and OH stretching modes, respectively. If the HOD reactant is in the ground vibrational state, i.e. (000), the abstraction of the H atom is preferred by a factor of more than 2, as shown in panel (a). This result can be explained by the different masses of the H and D atoms. Due to the lighter mass and the larger zero-point energy (ZPE), the H atom is easier to be abstracted than the D atom. In panel (c) where the OD stretching vibration is excited in the HOD reactant, i.e. (100), the situation is reversed: the abstraction of D is more favorable than the abstraction of H. This agrees with intuition and is quantitatively supported by the SVP model,<sup>59</sup> which yields a value of 0.96 in Table I for the (100) state of HOD in the HD + OH channel. This is readily understandable as the OD stretching vibration of HOD aligns well with the reaction coordinate at the transition state of the HD + OH channel. As a result, the excitation of the OD stretching vibration of HOD promotes the abstraction of D atom from the HOD reactant and dramatically increases the

reactivity. In the  $\text{H}_2 + \text{OD}$  channel, on the other hand, the OD bond behaves as a spectator and the reactivity is only slightly affected compared to the ground vibrational state. The reduction of the threshold in the  $\text{H}_2 + \text{OD}$  channel has been explained in a recent work by the tiny contribution of the OH stretching local-mode state in the (100) eigenstate.<sup>52</sup> In panel (e), the excitation of the OH stretching vibration of HOD, i.e. (001), is found to further increase the reactivity of the  $\text{H}_2 + \text{OD}$  channel while the reactivity of the other channel is almost unchanged. This is also in good agreement with intuitive expectation and the SVP values in Table I, as the OH stretching mode in HOD is well aligned with the reaction coordinate at the transition state leading to the  $\text{H}_2 + \text{OD}$  channel. These trends survive the summation of the partial waves. On the right column of Fig. 1, the total reactive integral cross sections (ICSs) essentially show similar branching between the two product channels.

Fig. 1 demonstrates the impact of selective excitation of the stretching vibrational modes on the bond cleavage. The results agree reasonably well with the experiment of Zare and coworkers at the collision energy of  $1.5 \text{ eV}$ .<sup>13</sup> The comparison of branching ratios of the two abstraction channels are listed in Table II, along with the previous quantum dynamical results of Fu and Zhang.<sup>41</sup> The two theoretical results are in good agreement with minor difference presumably resulting from the different sizes of the vibrational and rotational basis used to describe the non-reacting OH/OD fragment. The present state-to-state calculations with the RCB method could not afford a basis as large as that in the work of Fu and Zhang, which did not attempt to resolve product states. As shown in Table II, the experimental  $\sigma_{\text{OD}}/\sigma_{\text{OH}}$  product branching ratio of  $1.38 \pm 0.14:1$  for the ground vibrational state can be compared to the present theoretical value of 2.6:1. For

the OD and OH stretching excited states, the theoretical branching ratios fall within the estimated range of the experiment. Also shown in Table II are the variations of the branching ratio with respect to collision energy  $E_c$ . For the HOD reactant in the ground vibrational state,  $\sigma_{OD}/\sigma_{OH}$  is weakly dependent on  $E_c$ , because the ratio is largely determined by the different masses of the H and D atoms and the ZPE of the breaking bond. On the other hand, when the OH stretching mode is excited, the  $\sigma_{OD}/\sigma_{OH}$  branching ratio decreases with the increase of collision energy. This observation is not difficult to rationalize. The internal vibrational energy deposited in the OH vibration is fully utilized to facilitate the reaction by channeling almost all the energy into the reaction coordinate, while the translational energy is less efficient in this respect. The portion of the internal energy in the total energy decreases with the increase of collision energy. In analogy, this can also explain the change of the  $\sigma_{OD}/\sigma_{OH}$  branching ratio with respect to collision energy when OD stretching mode is excited.

Selective control of product channels by initial excitation of the stretching vibrations in the reactive bond is straightforward to understand based on the SVP model.<sup>67</sup> However, how the bending excitation affects the branching ratio is less studied.<sup>10, 15, 29, 41</sup> According to the SVP model,<sup>67</sup> the bending vibration should be less efficient in promoting the reaction (see Table I). In Fig. 2, total reaction probabilities and ICSs of the two product channels are compared for the HOD reactant in the first and second bending excited vibrational states. In accordance with the prediction of the SVP model, the excitation of the bending vibration has smaller enhancement than the stretching vibrations. Because the internal energy initially deposited in the bending vibration can only be partially and less efficiently channeled into the reaction coordinate during the reaction, reaction

probabilities in both channels are only slightly increased. When the HOD reactant is prepared in the first bending excited state, i.e. (010), the product branching ratios in Table II at different collision energies are similar to the ones for the ground vibrational state, which suggests that cleavage of either the OH or the OD bond of the HOD reactant is hardly affected by the bending excitation. This is intuitive: the bending mode is weakly coupled to the reaction coordinate at the transition state, which is along the stretching vibrational coordinate. In Table I, the bending mode has a SVP value of 0.15 for both product channels, which suggests the same promoting effect in the two product channels.

With the above understanding that the (010) vibrational state has similar and small enhancement in the two product channels, it is surprising to note the drastic change of the branching ratio when the HOD reactant is doubly excited in the bending mode. As shown in Fig. 2 (c) and (d), the (020) state enhances the reactivity in both product channels by reducing reaction threshold and increasing reaction probabilities and cross sections. However, the HD + OH channels is enhanced much more than the H<sub>2</sub> + OD one, resulting in a change of the branching ratio, as shown in Table II. While the HOD reactant in the (010) vibrational state has similar branching ratios as the (000) vibrational state and prefers to rupture the bond associated with the lighter H atom, it is interesting to note that the excitation of the (020) vibrational state changes the branching ratio by inclining to rupture the OD bond.

The origin of the drastic change of product branching ratio from the (010) to the (020) vibrational states stems from a 1:2 Fermi resonance between the OD stretching fundamental and the first bending overtone in HOD.<sup>68,69</sup> Because of their approximately equal excitation energies, the two members of the Fermi resonance pair are the mixtures

of two zero-order local-mode states. The mixing can be visualized in Figs. 3 (a) and (c), where the wavefunctions of the (100) and (020) eigenstates are plotted in the D+OH Jacobi coordinate system with the OH bond length ( $r$ ) fixed at its equilibrium geometry.  $R$  is the distance between D atom and the OH center of mass, and  $\theta$  is the angle between the OH bond and the  $\mathbf{R}$  vector. While the nodal structures of the two states are clearly visible in the respective vibrational coordinates, i.e., the O-D stretch and bend, the Fermi mixing manifests itself in the shapes of the wave functions. This is clearly shown that the mixing of the (020) state with the (100) state results in a curved shape along the bending coordinate. This mixing is also seen in the distorted wavefunction of the (100) state. The mode mixing can be quantitatively analyzed by investigating the representation of the vibrational eigenstates in the local-mode basis functions, which are direct products of three one-dimensional vibrational states: OD/OH stretching vibrational states and the bending vibrational states defined with one-dimensional cuts of the asymptotic HOD PES at the minimum. In Table III, the expansion coefficients of the five eigenstates in the local-mode bases are given. The local-mode basis functions are denoted as  $|(nm)b\rangle$ , where  $n$ ,  $m$ , and  $b$  are the quantum numbers of the OD stretching ( $R$ ), OH stretching ( $r$ ), and bending ( $\theta$ ) vibrations. The (000), (010), and (001) eigenstates are dominated by the  $|(00)0\rangle$ ,  $|(00)1\rangle$ , and  $|(01)0\rangle$  local-mode states, respectively, while Fermi resonance manifests itself by the mixing of the  $|(10)0\rangle$  and  $|(00)2\rangle$  local-mode states in the (100) and (020) eigenstates. With the expansion coefficients in Table III, the wave functions of the  $|(10)0\rangle$  and  $|(00)2\rangle$  local modes are obtained by linear combinations of the two eigenstates. In Figs. 3 (b) and (d), the local-mode wave functions have distinctive nodal structure without the distortion seen in the eigenstates. To this end, the enhancement of

the HD + OH channel by the excitation of the (020) modes can be explained by the  $|(10)0\rangle$  local-mode component in the (020) eigenstate. As shown in Fig. 1 (d) and Table II, the excitation of the OD stretching mode significantly enhances the HD + OH channel. Although there is only a  $\sim 11\%$   $|(10)0\rangle$  local-mode component in the (020) eigenstate, the large reactivity of the  $|(10)0\rangle$  local-mode component substantially promotes the HD + OH channel. The “reactivity borrowing” picture emerging from this analysis is quite similar to that discussed in the recent work of the  $\text{H} + \text{CHD}_3 \rightarrow \text{H}_2 + \text{CD}_3$  reaction.<sup>61</sup>

It is interesting to note that a recent full-dimensional state-to-state quantum dynamics study of the HD + OH channel in the title reaction revealed a startling observation that the excitation of the OH stretching vibration in the HOD reactant produced some purely vibrationless OH product at low collision energies.<sup>52</sup> This surprising observation appeared to violate the well-accepted spectator model for the non-reacting OH bond that the internal energy initially deposited in the OH bond should be sequestered throughout the reaction. Careful analysis within the local-mode regime revealed that the surprising reactivity is not due to vibrational non-adiabaticity during the reaction but to a small OD excited local-mode component, i.e.  $|(10)0\rangle$ , in the (001) reactant eigenstates. Here, the change of branching ratio by the excitation to the (020) eigenstate is explained by the same mechanism. The title reaction is a direct reaction with a reaction time scale of  $\sim 200$  fs. During this short period of reaction time, the non-adiabatic vibrational energy transfer is negligible. The fact that the mixing of the local-mode zero-order states exists already in the initial state of the reactant is analogous to the Fermi resonances discussed above. In other words, it is the static local-mode component in the initial wave function rather than the dynamic effect during reaction process that is responsible for the mode-specific

chemistry. We note in passing that this discovery is in accordance with the observation in the  $\text{H}+\text{H}_2\text{O}$  reaction where the ratio of the  $\text{OH}(\nu=1)$  and  $\text{OH}(\nu=0)$  products is approximately equal to the relative reactivity of the reactive OH bond in the  $\nu=0$  and  $\nu=1$  states.<sup>48</sup>

The change of the product branching ratio by the excitation of (020) mode is interesting and deserves a more detailed analysis at the state-to-state level. In Fig. 4, the OD and  $\text{H}_2$  product vibrational state resolved ICSs in the  $\text{H}_2 + \text{OD}$  channel are shown from ground vibrational state and the two bending excited vibrational states of the HOD reactant. In panels (a) and (b) with the reactant in the ground vibrational state, (000), both the OD and  $\text{H}_2$  products have no vibrational excitation in the collision energy range in the figure. With the excitation of the (010) vibrational state in panel (c), the OD product still has no vibrational excitation although the  $\text{OD}(\nu=1)$  vibrational state is energetically accessible. The non-reacting OD bond is well known to be a spectator and is decoupled from the reaction coordinate, as shown in Table I (the SVP value for the vibration of the OD product is negligible). It is thus not surprising to observe the absence of any OD vibrational excitation. On the other hand, the newly formed bond in the  $\text{H}_2$  product strongly couples with the reaction coordinate so that the post-transition state energy release can be effectively channeled to the excitation of  $\text{H}_2$  vibration when energy is available. In panel (d), it can be seen that the  $\text{H}_2(\nu=1)$  product vibrational state starts to be populated at the collision energy larger than 1.2 eV when energy exceeds the threshold of the  $\text{H}_2(\nu=1)$  product. In panels (f), the (020) state further reduces the threshold of the  $\text{H}_2(\nu=1)$  product. Surprisingly, the  $\text{OD}(\nu=1)$  product in panel (e) is observed, seemingly

violating the conclusion drawn from panel (c) that the non-reacting OD fragment is a spectator. This actually is the manifestation of Fermi resonance at the state-to-state level. Due to state-mixing, a  $|{(10)0}\rangle$  local-mode component exists in the  $(020)$  initial state. Thanks to the spectator behavior of OD, the excitation of the OD stretching vibration is able to be sequestered during the reaction and observed in the vibrational excitation in the OD product.

In Fig. 5, the OH and HD product vibrational state resolved ICSs are similarly analyzed in the HD + OH channel for the same three initial states of the HOD reactant. For all the three initial states, the OH product has no noticeable vibrational excitation throughout the energy range. This is jointly explained by two factors: (1) the absence of the coupling between the non-reacting OH bond and the reaction coordinate; (2) the absence of noticeable  $|{(01)0}\rangle$  local-mode state in all the three initial states. On the other hand, the HD( $\nu=1$ ) product vibrational state is dynamically excited due to its coupling to the reaction coordinate, which is in agreement with the SVP value in Table I.

#### IV. Conclusions

In the present work, it was shown that a Fermi resonance can significantly affect the product channel branching and product state distribution in a polyatomic reaction. The bond-selective chemistry of the H + HOD reaction mostly follows intuitive expectation and quantitative sudden models. The calculated branching ratios agree well with the existing experimental results for ground, fundamental OD stretching and OH stretching excited vibrational states of the HOD reactant. The HOD reactant in the ground vibrational state is more likely to react through the OH than the OD bond due to the different masses and ZPEs. An important exception is found for the bending excited

modes. While the fundamental excitation of the bending mode has a similar product branching to the ground vibrational state, the excitation of the first overtone of bending mode results in a significant enhancement in the HD + OH channel due to the 1:2 Fermi resonance between the fundamental OD stretch and the first overtone of the bend .

The present work underlines the necessity of a careful initial state analysis if the quantum reaction dynamics are studied at the state-to-state level. To provide an accurate quantum mechanical analysis of a chemical reaction, it is very important to distinguish the static and dynamical contributions of a zero-order local-mode state to the product state distribution. Static state mixing caused by Fermi resonance in the initial state affects the intuitive interpretation of the mode-specific chemistry. Without recognizing the static contribution, one might easily misinterpret the static contribution as results of dynamic processes during the reaction.

Finally, it is interesting to point out that a Fermi resonance is intrinsic to the molecule. However, mixed states may be prepared by a coherent excitation of nearby vibrational modes using a short pulse laser. Such coherent states can be viewed as an artificial Fermi resonance, and thus they might be used to control the product branching even when an intrinsic Fermi resonance is absent.

**Electronic Supplementary Information (ESI)** available: Theoretical details used in the calculations. See DOI: 10.1039/x0xx00000x

### **Acknowledgements**

Z.B. and U.M. thank Alexander von Humboldt-Stiftung for a Fellowship. Z.B. thanks Prof. Zhigang Sun for the computing resources. H.G. thanks the Department of Energy

(Grant No. DE-SC0015997) for partial support. Z.B. and H.G. thank Prof. Kopin Liu for discussion.

**Reference:**

1. R. N. Zare, *Science*, 1998, **279**, 1875-1879.
2. F. F. Crim, *Proc. Natl. Acad. Sci. U.S.A.*, 2008, **105**, 12654-12661.
3. K. Liu, *Annu. Rev. Phys. Chem.*, 2016, **67**, 91-111.
4. F. F. Crim, *Acc. Chem. Res.*, 1999, **32**, 877-884.
5. D. H. Zhang and H. Guo, *Annu. Rev. Phys. Chem.*, 2016, **67**, 135-158.
6. B. Zhao and H. Guo, *Wiley Interdiscip. Rev. Comput. Mol. Sci.*, 2017, **7**, 1301.
7. J. Li, B. Jiang, H. Song, J. Ma, B. Zhao, R. Dawes and H. Guo, *J. Phys. Chem. A*, 2015, **119**, 4667-4687.
8. B. Fu, X. Shan, D. H. Zhang and D. C. Clary, *Chem. Soc. Rev.*, 2017, **46**, 7625-7649.
9. A. Sinha, M. C. Hsiao and F. F. Crim, *J. Chem. Phys.*, 1990, **92**, 6333-6335.
10. A. Sinha, M. C. Hsiao and F. F. Crim, *J. Chem. Phys.*, 1991, **94**, 4928-4935.
11. R. B. Metz, J. D. Thoemke, J. M. Pfeiffer and F. F. Crim, *J. Chem. Phys.*, 1993, **99**, 1744-1751.
12. M. J. Bronikowski, W. R. Simpson, B. Girard and R. N. Zare, *J. Chem. Phys.*, 1991, **95**, 8647-8648.
13. M. J. Bronikowski, W. R. Simpson and R. N. Zare, *J. Phys. Chem.*, 1993, **97**, 2194-2203.
14. A. Sinha, J. D. Thoemke and F. F. Crim, *J. Chem. Phys.*, 1992, **96**, 372-376.
15. M. J. Bronikowski, W. R. Simpson and R. N. Zare, *J. Phys. Chem.*, 1993, **97**, 2204-2208.
16. I. W. M. Smith and F. Fleming Crim, *Phys. Chem. Chem. Phys.*, 2002, **4**, 3543-3551.
17. B. R. Strazisar, C. Lin and H. Floyd Davis, *Science*, 2000, **290**, 958-961.
18. S. Liu, C. L. Xiao, T. Wang, J. Chen, T. G. Yang, X. Xu, D. H. Zhang and X. M. Yang, *Faraday Discuss.*, 2012, **157**, 101-111.
19. C. L. Xiao, X. Xu, S. Liu, T. Wang, W. R. Dong, T. G. Yang, Z. G. Sun, D. X. Dai, X. Xu, D. H. Zhang and X. M. Yang, *Science*, 2011, **333**, 440-442.
20. F. Matzkies and U. Manthe, *J. Chem. Phys.*, 1998, **108**, 4828-4836.
21. U. Manthe, T. Seideman and W. H. Miller, *J. Chem. Phys.*, 1994, **101**, 4759-4768.
22. U. Manthe, T. Seideman and W. H. Miller, *J. Chem. Phys.*, 1993, **99**, 10078-10081.
23. U. Manthe and F. Matzkies, *J. Chem. Phys.*, 2000, **113**, 5725-5731.
24. D. Neuhauser, *J. Chem. Phys.*, 1994, **100**, 9272-9275.
25. J. Dai, W. Zhu and J. Z. H. Zhang, *J. Phys. Chem.*, 1996, **100**, 13901-13903.
26. W. Zhu, J. Q. Dai, J. Z. H. Zhang and D. H. Zhang, *J. Chem. Phys.*, 1996, **105**, 4881-4884.
27. D. H. Zhang and J. C. Light, *J. Chem. Phys.*, 1996, **104**, 4544-4553.
28. D. H. Zhang and J. C. Light, *J. Chem. Phys.*, 1996, **105**, 1291-1294.
29. D. H. Zhang and J. C. Light, *J. Chem. Soc. Faraday Trans.*, 1997, **93**, 691-697.
30. D. H. Zhang, M. A. Collins and S. Y. Lee, *Science*, 2000, **290**, 961-963.
31. D. H. Zhang, M. H. Yang and S. Y. Lee, *J. Chem. Phys.*, 2001, **114**, 8733-8736.
32. D. H. Zhang, M. H. Yang and S. Y. Lee, *Phys. Rev. Lett.*, 2002, **89**.
33. E. M. Goldfield and S. K. Gray, *J. Chem. Phys.*, 2002, **117**, 1604-1613.
34. P. Defazio and S. K. Gray, *J. Phys. Chem. A*, 2003, **107**, 7132-7137.
35. J. Mayneris, M. González and S. K. Gray, *Comp. Phys. Comm.*, 2008, **179**, 741-747.
36. M. T. Cvitaš and S. C. Althorpe, *J. Phys. Chem. A*, 2009, **113**, 4557-4569.
37. M. T. Cvitas and S. C. Althorpe, *J. Chem. Phys.*, 2011, **134**, 024309.
38. M. T. Cvitas and S. C. Althorpe, *J. Chem. Phys.*, 2013, **139**, 064307.
39. B. Jiang, D. Xie and H. Guo, *J. Chem. Phys.*, 2011, **135**, 084112.
40. D. H. Zhang, *J. Chem. Phys.*, 2006, **125**.

41. B. Fu and D. H. Zhang, *J. Chem. Phys.*, 2015, **142**, 064314.
42. B. Fu and D. H. Zhang, *J. Chem. Phys.*, 2013, **138**, 184308.
43. B. Zhao, Z. Sun and H. Guo, *J. Chem. Phys.*, 2014, **141**, 154112.
44. B. Zhao, Z. Sun and H. Guo, *J. Am. Chem. Soc.*, 2015, **137**, 15964-15970.
45. B. Zhao, Z. Sun and H. Guo, *J. Chem. Phys.*, 2016, **144**, 064104.
46. B. Zhao, Z. Sun and H. Guo, *J. Chem. Phys.*, 2016, **144**, 214303.
47. S. Liu, X. Xu and D. H. Zhang, *J. Chem. Phys.*, 2012, **136**, 144302.
48. S. Liu and D. Zhang, *Chem. Sci.*, 2015, **7**, 261-265.
49. Z. Zhao, S. Liu and D. H. Zhang, *J. Chem. Phys.*, 2016, **145**, 134301.
50. B. Zhao, Z. Sun and H. Guo, *J. Chem. Phys.*, 2016, **145**, 134308.
51. B. Zhao, Z. Sun and H. Guo, *J. Chem. Phys.*, 2016, **145**, 184106.
52. B. Zhao, Z. Sun and H. Guo, *Phys. Chem. Chem. Phys.*, 2018, **20**, 191-198.
53. K. Kudla and G. C. Schatz, *Chem. Phys. Lett.*, 1992, **193**, 507-511.
54. J. M. Bowman and D. Wang, *J. Chem. Phys.*, 1992, **96**, 7852-7854.
55. D. Wang and J. M. Bowman, *J. Chem. Phys.*, 1993, **98**, 6235-6247.
56. G. Nyman and D. C. Clary, *J. Chem. Phys.*, 1993, **99**, 7774-7786.
57. B. Jiang and H. Guo, *J. Chem. Phys.*, 2013, **138**, 234104.
58. J. C. Polanyi, *Science*, 1987, **236**, 680-690.
59. H. Guo and B. Jiang, *Acc. Chem. Res.*, 2014, **47**, 3679-3685.
60. H. Guo and K. Liu, *Chem. Sci.*, 2016, **7**, 3992-4003.
61. R. Ellerbrock and U. Manthe, *J. Chem. Phys.*, 2017, **147**, 241104.
62. B. Jiang and H. Guo, *J. Chin. Chem. Soc.*, 2014, **61**, 847-859.
63. S. Gomez-Carrasco and O. Roncero, *J. Chem. Phys.*, 2006, **125**, 054102.
64. Z. G. Sun, H. Guo and D. H. Zhang, *J. Chem. Phys.*, 2010, **132**.
65. M. D. Feit, J. A. Fleck Jr. and A. Steiger, *J. Comput. Phys.*, 1982, **47**, 412-433.
66. J. Chen, X. Xu, X. Xu and D. H. Zhang, *J. Chem. Phys.*, 2013, **138**, 154301.
67. B. Jiang and H. Guo, *J. Am. Chem. Soc.*, 2013, **135**, 15251-15256.
68. J. R. Reimers and R. O. Watts, *Mol. Phys.*, 1984, **52**, 357-381.
69. W. S. Benedict, N. Gailar and E. K. Plyler, *J. Chem. Phys.*, 1956, **24**, 1139-1165.

Table I. SVP values of the H + HOD reaction for both the H<sub>2</sub> + OD and the HD + OH product channels.

	SVP values			
	Reactant		Product	
H <sub>2</sub> + OD product channel	Bend	0.15	H <sub>2</sub> vib.	0.37
	OD stretch	0.06		
	OH stretch	0.93	OD vib.	0.02
	Trans.	0.33		
HD + OH product channel	Bend	0.15	HD vib.	0.29
	OD stretch	0.96		
	OH stretch	0.03	OH vib.	0.01
	Trans.	0.28		

Table II. ICS branching ratio of the  $\text{H}_2 + \text{OD}$  channel over the  $\text{HD} + \text{OH}$  channel for five vibrational initial states of the HOD reactants at six different collision energies.

$E_c$ (eV)	Branching ratio: $\sigma_{\text{OD}}/\sigma_{\text{OH}}$							FZ@1.5 <sup>41</sup>	Exp.@1.5 <sup>13</sup>
	1.0	1.1	1.2	1.3	1.4	1.5			
(000)	2.3:1	2.1:1	2.2:1	2.3:1	2.5:1	2.6:1	2.5:1	1.38±0.14:1	
(010)	2.9:1	2.7:1	2.7:1	2.7:1	2.8:1	2.8:1			
(100)	1:15.6	1:12.2	1:9.7	1:7.9	1:6.6	1:5.5	1:6.9	<1:5.8, >1:24	
(020)	0.8:1	0.9:1	1.0:1	1.1:1	1.2:1	1.3:1			
(001)	176.3:1	123.7:1	90.8:1	70.6:1	57.1:1	47.1:1	47:1	>25:1	

Table III. Weights of local-mode bases in the five vibrational eigenstates of the HOD reactant, along with the vibrational frequencies. The initial state  $\psi_i$  is written as a linear combination of the local-mode bases, i.e.  $\psi_i = \sum C_{nmb}|(nm)b\rangle$ , where  $n$ ,  $m$ , and  $b$  are the quantum numbers of the OD stretching, OH stretching, and bending vibrations.

$(v_{OD}, v_b, v_{OH})$	Vib. Energy ( $\text{cm}^{-1}$ )		$ C_{nmb} ^2$				
	Theory	Exp. <sup>69</sup>	$ (00)0\rangle$	$ (00)1\rangle$	$ (00)2\rangle$	$ (10)0\rangle$	$ (01)0\rangle$
(000)	0.0	0.0	0.992	0.003	0.000	0.004	0.000
(010)	1391.1		0.003	0.970	0.006	0.002	0.002
(100)	2720.6	2723.7	0.006	0.004	0.097	0.867	0.004
(020)	2764.9	2782.2	0.001	0.004	0.847	0.107	0.000
(001)	3697.1	3707.5	0.001	0.003	0.000	0.002	0.973

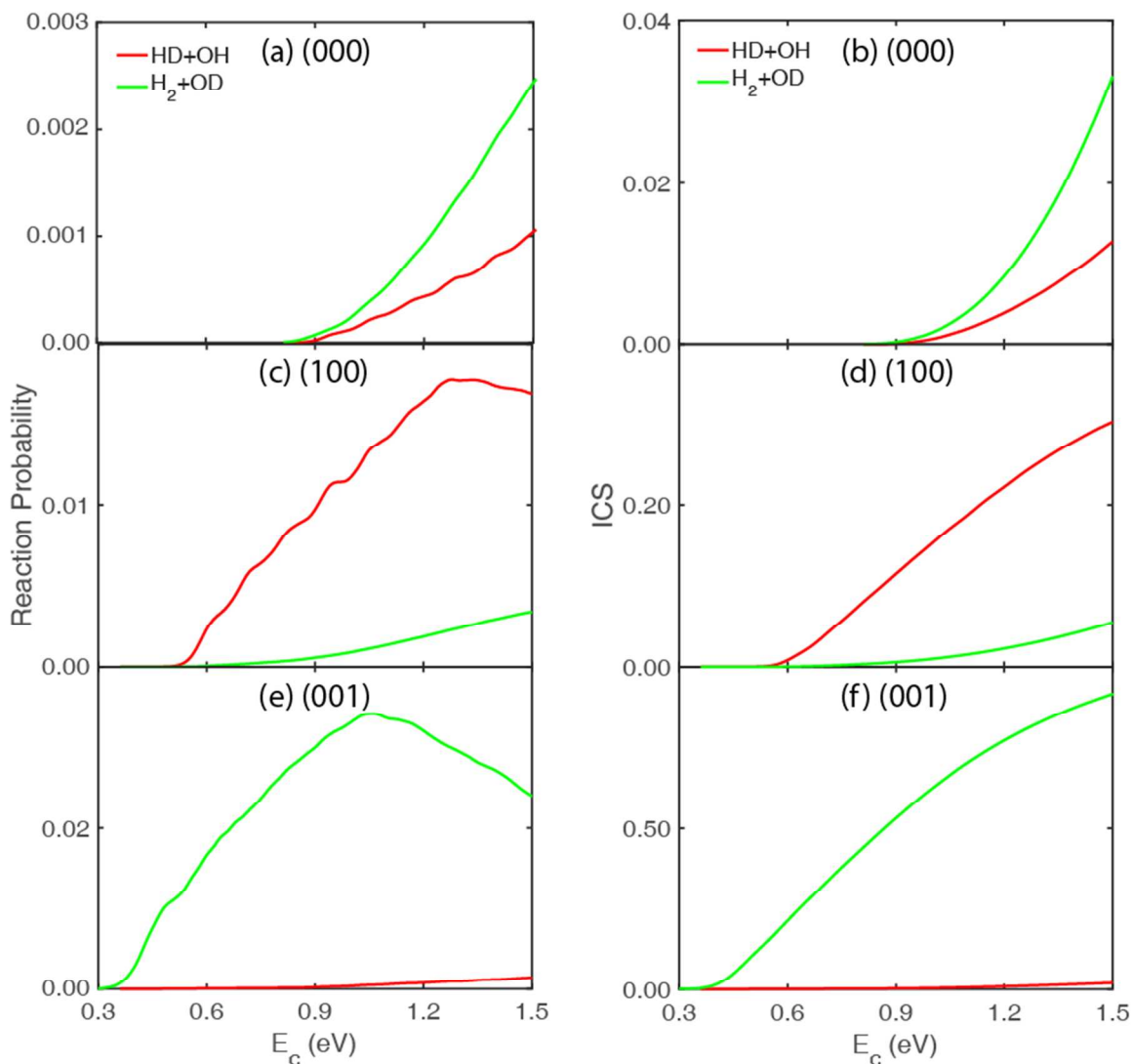


Fig. 1 Total reaction probabilities (left column) and ICSs (right column) of the HD + OH (red) and H<sub>2</sub> + OH (green) product channels of the title reaction from three initial states of the HOD reactant: (a) and (b) ground vibrational state (000), (c) and (d) OD stretching excited vibrational state (100), (e) and (f) OH stretching excited vibrational state (001). Note that the reaction probabilities and ICSs of different initial states are plotted in different scales.

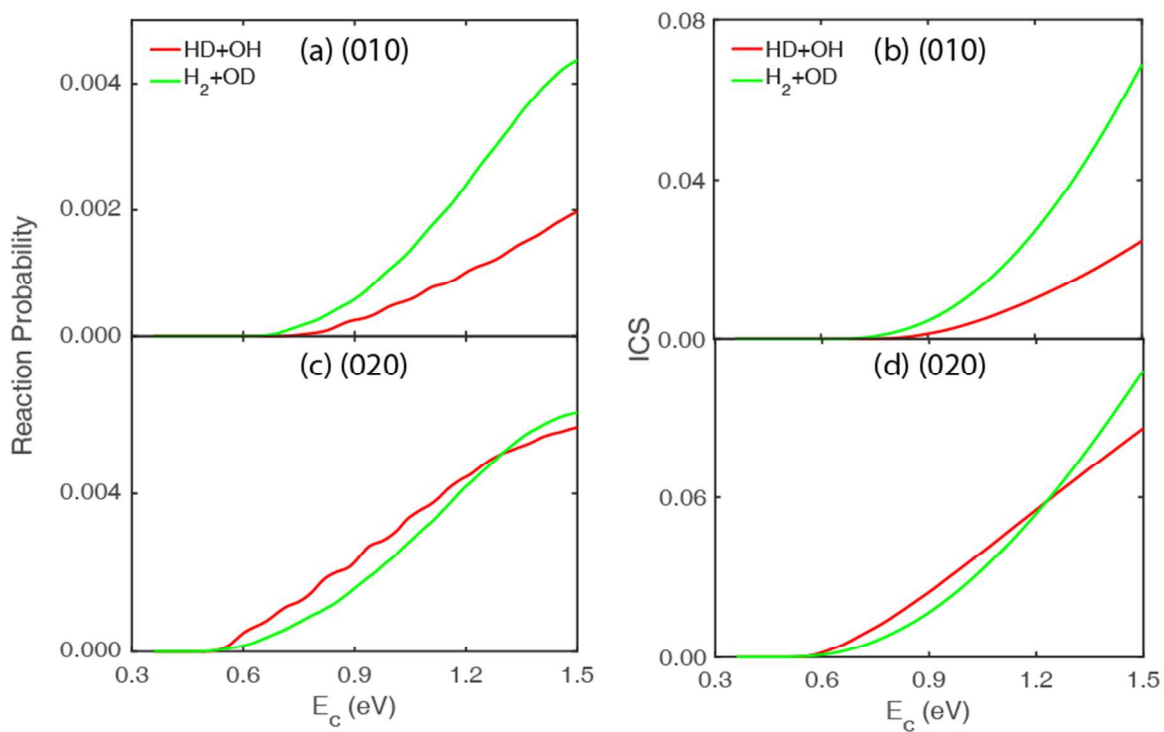


Fig. 2 Same as Fig.1 except from two different initial states of the HOD reactant: (a) and (b) first bending excited vibrational state (010), and (c) and (d) second bending excited vibrational state (020). Note that the reaction probabilities and ICSs of different initial states are plotted in different scales.

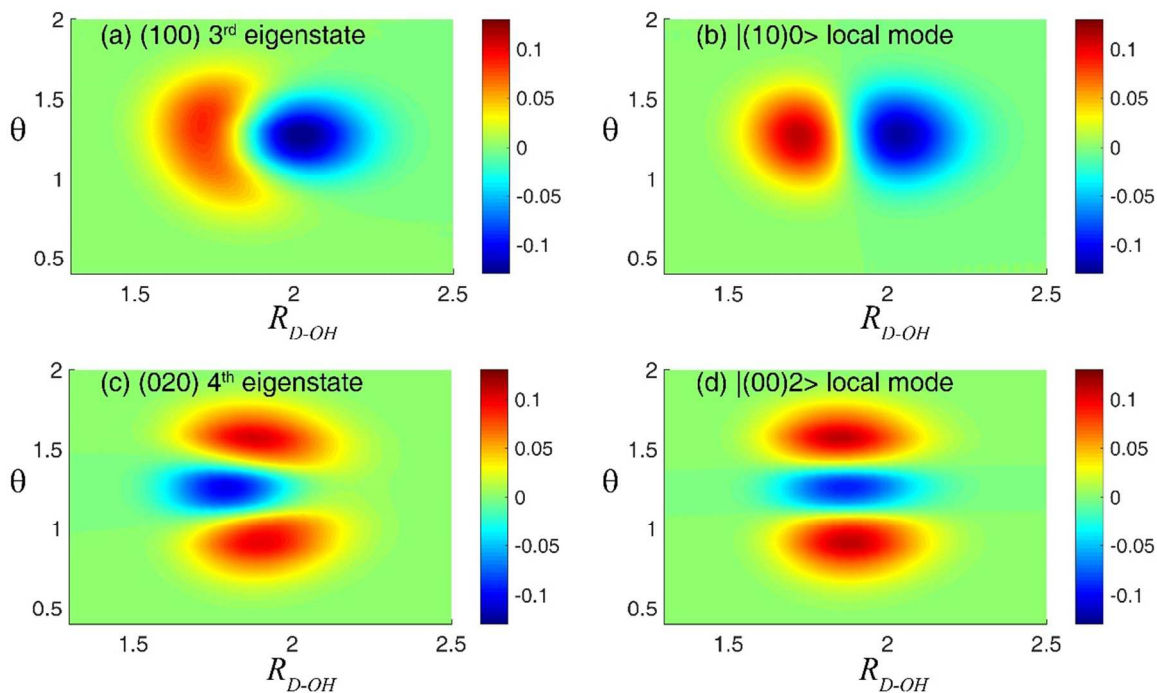


Fig. 3 Two-dimensional (2D) contour plots of the vibrational states of the HOD reactant in the D + OH Jacobi coordinate system, where  $R$  is the distance between D atom and the OH center of mass, and  $\theta$  is the angle between the OH bond and the  $\mathbf{R}$  vector. The bond length of the non-reacting OH bond ( $r$ ) is fixed at its equilibrium value. The two eigenstates in Fermi resonance: (a) the (100) eigenstate and (c) the (020) eigenstate, and the two corresponding local-mode states: (b) the |(10)0> local mode and (d) the |(00)2> local mode.

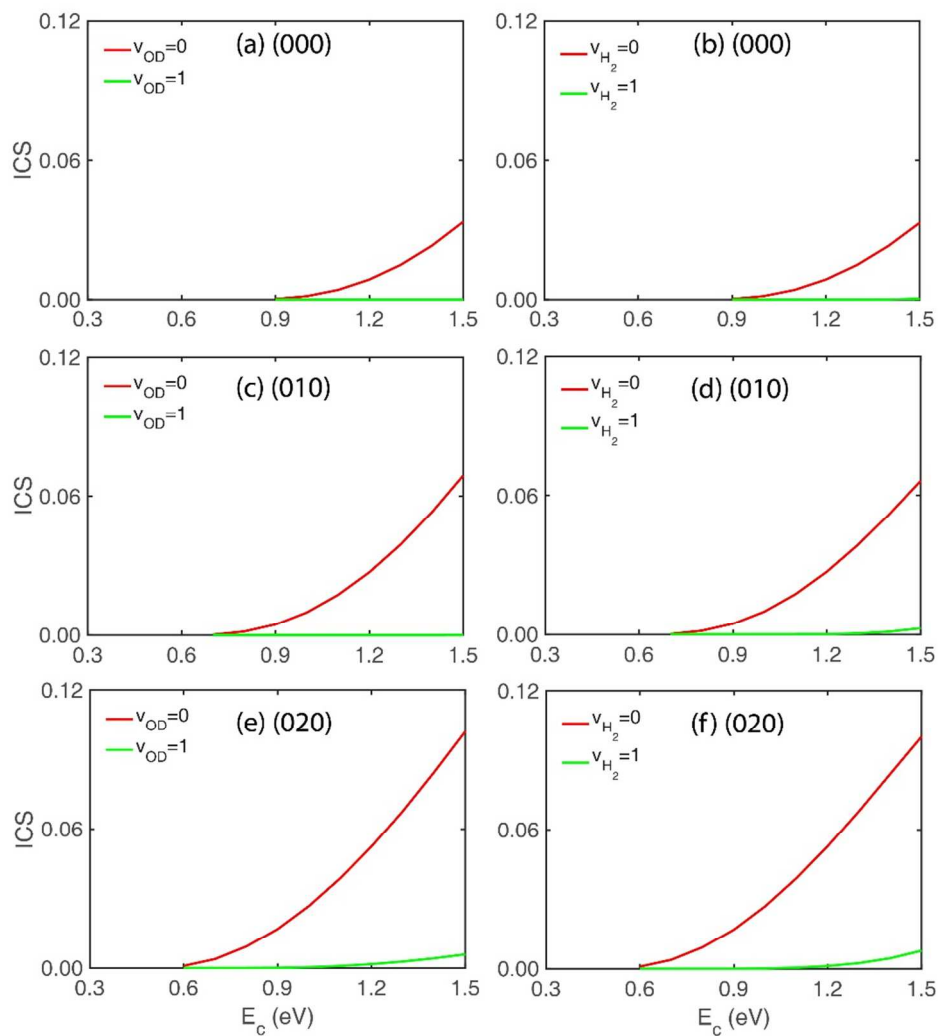


Fig. 4 OD (left column) and  $H_2$  (right column) product vibrational state resolved ICSs in the  $H_2 + OD$  channel from three initial states of the HOD reactant with respect to collision energy: (a) and (b) ground vibrational state (000), (c) and (d) first bending excited vibrational state (010), and (e) and (f) second bending excited vibrational state (020). The rotational state populations of the  $H_2$  and OD products are summed.

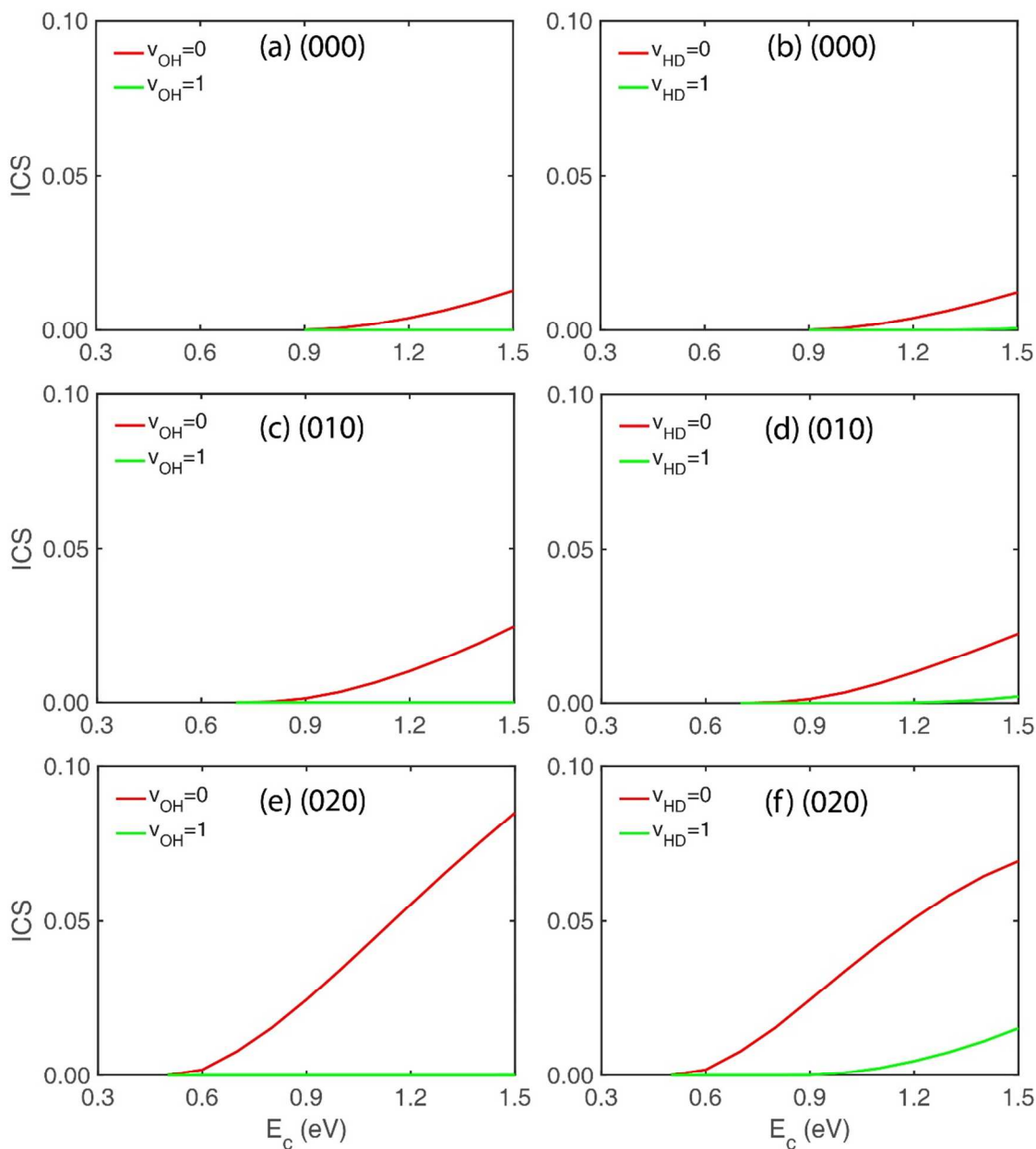
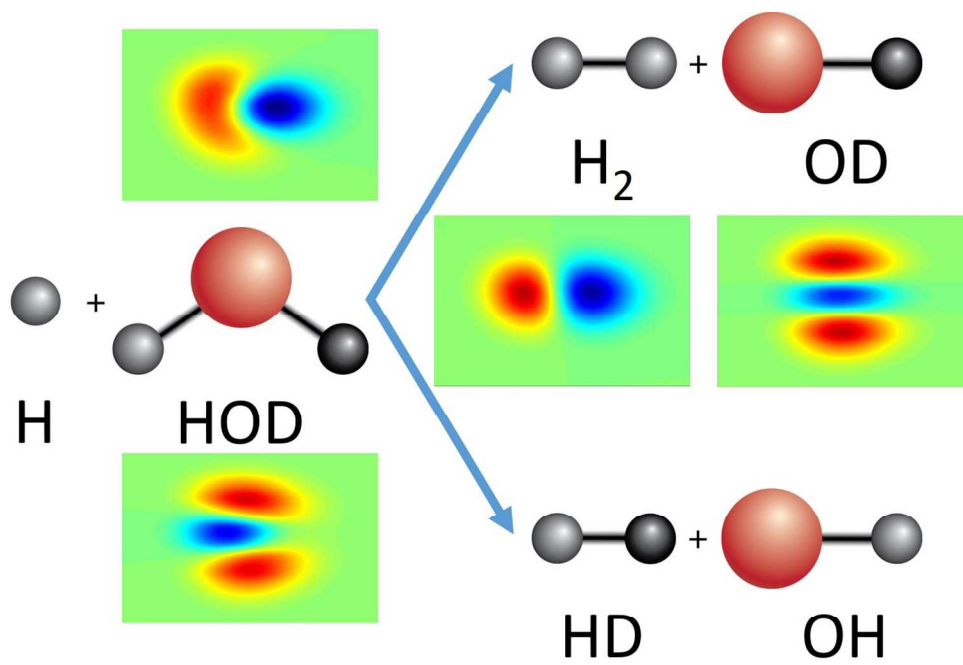


Fig. 5 OH (left column) and HD (right column) product vibrational state resolved ICSs in the HD + OH channel from three initial states of the HOD reactant with respect to collision energy: (a) and (b) ground vibrational state (000), (c) and (d) first bending excited vibrational state (010), and (e) and (f) second bending excited vibrational state (020). The rotational state populations of the HD and OH products are summed.



248x174mm (150 x 150 DPI)